

**Citation for published version:**

Farbod Khoshnoud, Yuchi Zhang, Ray Shimura, Amir Shahba, Guangming Jin, Georgios Pissanidis, Yong K. Chen, and Clarence W. De Silva, 'Energy Regeneration From Suspension Dynamic Modes and Self-Powered Actuation', *IEEE/ASME Transactions on Mechatronics*, Vol. 20 (5): 2513-2524, October 2015.

**DOI:**

<https://doi.org/10.1109/TMECH.2015.2392551>

**Document Version:**

This is the Accepted Manuscript version.

The version in the University of Hertfordshire Research Archive may differ from the final published version.

**Copyright and Reuse:**

© 2015 IEEE

Personal use of this material is permitted. Permission from IEEE must be obtained for all other uses, in any current or future media, including reprinting/republishing this material for advertising or promotional purposes, creating new collective works, for resale or redistribution to servers or lists, or reuse of any copyrighted component of this work in other works.

**Enquiries**

If you believe this document infringes copyright, please contact Research & Scholarly Communications at [rsc@herts.ac.uk](mailto:rsc@herts.ac.uk)

# Energy regeneration from suspension dynamic modes and self-powered actuation

Farbod Khoshnoud, Yuchi Zhang, Ray Shimura, Amir Shahba, Guangming Jin, Georgios Pissanidis, Yong K. Chen, Clarence W. De Silva, *Fellow, IEEE*

**Abstract**—This paper concerns energy harvesting from vehicle suspension systems. The generated power associated with bounce, pitch and roll modes of vehicle dynamics is determined through analysis. The potential values of power generation from these three modes are calculated. Next, experiments are carried out using a vehicle with a four jack shaker rig to validate the analytical values of potential power harvest. For the considered vehicle, maximum theoretical power values of 1.1kW, 0.88kW and 0.97kW are associated with the bounce, pitch and roll modes, respectively, at 20 Hz excitation frequency and peak to peak displacement amplitude of 5 mm at each wheel, as applied by the shaker. The corresponding experimentally power values are 0.98kW, 0.74kW and 0.78kW. An experimental rig is also developed to study the behavior of regenerative actuators in generating electrical power from kinetic energy. This rig represents a quarter-vehicle suspension model where the viscous damper in the shock absorber system is replaced by a regenerative system. The rig is able to demonstrate the actual electrical power that can be harvested using a regenerative system. The concept of self-powered actuation using the harvested energy from suspension is discussed with regard to applications of self-powered vibration control. The effect of suspension energy regeneration on ride comfort and road handling is presented in conjunction with energy harvesting associated with random road excitations.

**Index Terms**—Energy harvesting, regenerative actuators, self-powered systems, vehicle dynamics.

## I. INTRODUCTION

THE level of power available for harvesting from vehicle suspension systems is reported to be in the range of 10's

This work was supported by the UK Defence Science and Technology Laboratory under Grant Contract No. DSTLX-1000076834.

Farbod Khoshnoud is with the Department of Mechanical Engineering, Brunel University, Uxbridge UB8 3PH, UK, (e-mail: Farbod.Khoshnoud@brunel.ac.uk).

Yuchi Zhang was with the University of Hertfordshire, now with Ford Motor Research & Engineering (Nanjing) Co. Ltd., No. 118 General Road, Jiangning Development Zone, Nanjing, China (e-mail: yzhan238@ford.com).

Ray Shimura, Amir Shahba and Guangming Jin were with the School of Engineering, University of Hertfordshire, Hatfield, AL10 9AB, UK.

Georgios Pissanidis is with the School of Engineering, University of Hertfordshire, Hatfield, AL10 9AB, UK (e-mail: g.l.pissanidis@herts.ac.uk).

Yong K. Chen is with the School of Engineering, University of Hertfordshire, Hatfield, AL10 9AB, UK (e-mail: y.k.Chen@herts.ac.uk).

Clarence W. De Silva is with the Department of Mechanical Engineering, University of British Columbia, Vancouver, BC, V6T 1Z4, Canada (e-mail: desilva@mech.ubc.ca).

to 1000's of Watts [1]-[12] depending on the vehicle type and testing conditions. In a typical shock absorber of a vehicle, the kinetic energy due to vertical oscillations is dissipated in the viscous dampers. This wasted energy can be recovered by replacing the viscous dampers with regenerative actuators. A regenerative actuator can harvest the kinetic energy, which can then be stored as electrical energy. The stored energy can be used for various purposes in the vehicle including active control of vibrations. In this case the regenerative actuator provides a self-powered system, which uses harvested energy to control its own actuation [13]-[16].

A regenerative actuator used for energy recovery in a suspension system can be a DC linear motor. The actuator acts as a power generator when a mechanical load is applied to it and can act as an actuator when voltage is applied. Such a system can also provide better vibration isolation than with a passive or a semi-active system when is utilized as a vibration control system [13]-[18]. The concept of an actuator in which energy storage elements is part of the actuator, and absorbs power, can be used for motion control [19]-[21].

Various novel systems have been designed for energy harvesting by other researchers. For instance, the use the rotation of the axle as input with a system placed around the axle, the motion can be transmitted to the generator through friction wheels [22]. This system is capable of producing more than 100 Watts of power at a simulated 55 mph. Motion-based energy harvesting devices are employed to road and railroad applications where the railroad devices are designed for generating energy from smaller displacement motions than the road vehicles [23]-[24]. A hydraulic pumping regenerative suspension can harvest energy from vibration while providing variable damping by controlling the electrical load of the energy recovery system [25]. Hydraulic-Electrical Energy Regenerative Suspension (HEERS) systems can provide similar characteristics as traditional shock absorbers where the parameters influencing on the performance of HEERS are found to be the hydraulic motor displacement, orifice area of check valve, inner diameter of pipelines, and charging pressure of accumulator [26]. Gain-scheduling control of electromagnetic regenerative shock absorbers can provide a solution where the parameters can be calibrated and directly related to the energy harvesting specifications [27].

The authors have reported the theoretical and experimental levels of harvested energy associated with the single degree-of-freedom (DOF) bounce mode of vehicle dynamics [28]. In

Section II of the present paper, the theory of energy harvesting is extended to the two DOF bounce, pitch and roll dynamics of a vehicle, and in Section III an experimental investigation is carried out on a Ford Focus vehicle using a four jack shaker rig for obtaining the potential amount of energy that can be harvested from an actual vehicle associated with the dynamic modes of the vehicle explored in the theory section (Section II). In Section IV, the actual amount of energy (not potential) that can be generated using a regenerative shock absorber is studied. Section V discusses the application of regenerative shock absorbers for a vehicle suspension system as a self-powered actuation system and as a power generation system. Section VI discusses the effect of energy extraction on ride comfort and road handling. This section also presents the analysis of energy extraction associated with real random road profiles. The following section gives the theory of energy harvesting associated with various modes of vehicle dynamics.

## II. THEORETICAL ANALYSIS OF HARVESTED ENERGY

The potential amount of energy that can be harvested associated with bounce, pitch and roll modes of vehicles is investigated in this section. This can represent the physical limits of the system in terms of the maximum amount of energy that can be harvested from suspension vibrations, if there is no energy loss in the energy harvester system. The dynamic modes of vibration is the fundamental topic in vehicle dynamics and therefore exploring the amount of energy associated with these dynamic modes as a potential power source for the vehicle is of significant importance.

### A. The Bounce Mode

The equation of motion of a mass-spring-damper model associated with the single degree-of-freedom bounce mode of vehicle dynamics can be expressed by

$$m\ddot{z} + c\dot{z} + kz = m\ddot{y} \quad (1)$$

where  $m$  = mass,  $c$  = damping constant,  $k$  = stiffness,  $y$  = displacement of the wheel from the road profile (input excitation), and  $z = x - y$  is the displacement of the mass relative to the wheel, where  $x$  is the displacement of the mass.

Consider a harmonic excitation of  $y = Y\sin\omega t$ , where  $\omega$  = frequency of excitation, and  $t$  = time. The steady state response may be expressed as  $z = Z\sin(\omega t - \phi)$ , where  $Z$  is the amplitude of the motion.

The kinetic energy in a vehicle shock absorber, which is usually dissipated, can be recovered using a regenerative mechanism that converts the kinetic energy to usable electrical energy. In this section it is assumed that the damper is replaced with a lossless energy harvester that can convert the kinetic energy due to vibration to useful means of energy source such as electrical energy stored in a battery.

The power in a damper is equal to the damping force times the relative velocity of the wheel and the mass,  $\dot{z}$ , expressed as ([28] and [30])

$$P = c\dot{z} \times \dot{z} \quad (2)$$

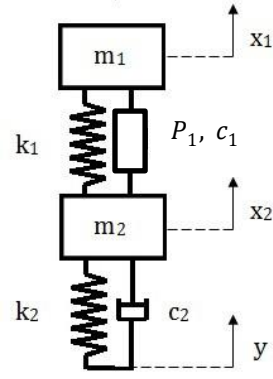


Fig. 1. The two-degree-of-freedom bounce model.

The single degree of freedom bounce mode discussed above can be extended to a two-degree-of-freedom (2DOF) model as in Fig. 1. In this figure,  $m_1$  = mass of quarter car, and  $m_2$  = mass of the tire. Also,  $k_1$  and  $k_2$  are the stiffness values of the spring of suspension and the tire, respectively, and  $c_1$  and  $c_2$  are the damping values of suspension and tire, respectively.

The power that can be harvested in this system when the damper  $c_1$  is replaced by a regenerative system is obtained next. Using the equation of motion of the 2DOF model in Fig. 1, and assuming  $x_1 = X_1e^{j\omega t}$ ,  $x_2 = X_2e^{j\omega t}$ ,  $y = Ye^{j\omega t}$ , the power output of the 2DOF can be obtained as:

$$P_1 = \frac{c_1\omega^2|Z_1|^2}{2} = \frac{c_1\omega^2}{2}(|X_1 - X_2|)^2 \quad (3)$$

where  $z_1 = x_1 - x_2$ ,  $Z_1 = X_1 - X_2$ , and  $X_1$  and  $X_2$  are the displacement amplitudes of  $m_1$  and  $m_2$ , respectively,  $Y$  = displacement excitation amplitude at the base, and  $\omega$  = excitation frequency.

### B. The Pitch Mode

The 2DOF pitch model of a vehicle is presented in Fig. 2. In this figure,  $x$  = displacement of the vehicle body and  $\theta$  = angular displacement about the center of gravity. The parameters  $a$  and  $b$  are the distances from the center of gravity to front wheel and rear wheel, respectively. Also,  $k_1$  and  $c_1$  are the stiffness and damping values of front suspension respectively, and  $k_2$  and  $c_2$  denote the corresponding rear suspension parameters. The input excitations at the front and rear wheels are  $y_1$  and  $y_2$ , respectively.

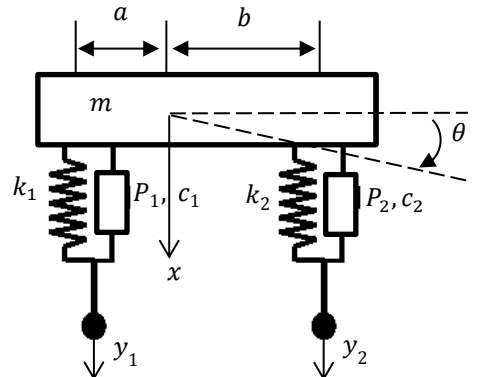


Fig. 2. The two-degree-of-freedom pitch model.

By writing the equation of motion of the 2DOF pitch model of a half vehicle shown in Fig. 2, and assuming harmonic excitations,  $y_1 = Y_1 e^{j\omega t}$ ,  $y_2 = Y_2 e^{j\omega t}$ , the displacements can be expressed as  $x = X e^{j\omega t}$ ,  $\theta = \phi e^{j\omega t}$ , where  $Y_1$  and  $Y_2$  are the amplitudes of the harmonic excitations applied on the front and rear wheels, respectively,  $X$  = amplitude of displacement, and  $\phi$  = angular displacement response in steady state.

By substituting the displacement amplitudes in the 2DOF equation of motion of the pitch mode and solving the equation for the displacement amplitudes, one obtains

$$X = \frac{\Delta_1}{\Delta_0} \text{ and } \phi = \frac{\Delta_2}{\Delta_0} \quad (4)$$

where  $\Delta_0$ ,  $\Delta_1$  and  $\Delta_2$  are obtained by Cramer's Rule. By assuming the relative displacements  $z_1$  and  $z_2$  as

$$z_1 = x - a\theta - y_1 \text{ and } z_2 = x + b\theta - y_2,$$

the total potential value of power output is obtained by adding the power generated in each suspension (the front wheel,  $P_1$ , and the rear wheel,  $P_2$ ) as

$$P_{Total} = P_1 + P_2 = \frac{c_1 \omega^2}{2} \left( \left| \frac{\Delta_1}{\Delta_0} - a \frac{\Delta_2}{\Delta_0} - Y_1 \right| \right)^2 + \frac{c_2 \omega^2}{2} \left( \left| \frac{\Delta_1}{\Delta_0} + b \frac{\Delta_2}{\Delta_0} - Y_2 \right| \right)^2 \quad (5)$$

The damping parameters  $c$ , used in the above equations, are the equivalent damping parameters correspond to the motor constant of the regenerative actuator, when the viscous damper is replaced by a regenerative system for energy harvesting applications. The relationship between the equivalent viscous damping of the shock absorber and the motor constant of the electromagnetic regenerative suspension is discussed in Section V.

### C. The Roll Mode

If  $a = b$ ,  $k_1 = k_2$ , and  $c_1 = c_2$  in Fig. 2 then it will represent the roll mode of vehicle dynamics. Therefore, the process in section B can be repeated when using  $a = b$ ,  $k_1 = k_2$ , and  $c_1 = c_2$  in the equations in order to obtain the power output corresponding to the roll mode.

The above dynamic models are simplified model of the seven-degree-of-freedom vehicle dynamic model [31]. Fig. 3 shows the power generated associated with bounce, pitch and roll modes of vehicle dynamics. For the roll mode we have  $a = b$ ,  $k_1 = k_2$ , and  $c_1 = c_2$  in Equation (5).

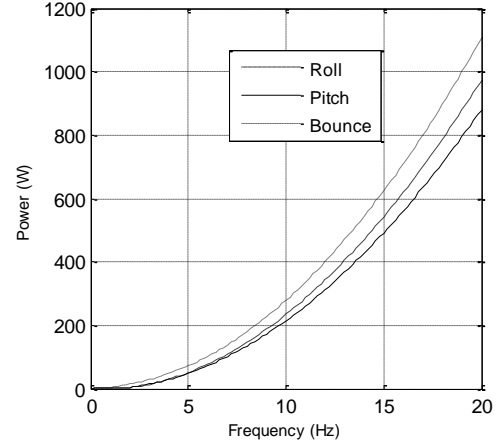


Fig. 3. The generated power versus the excitation frequency, for the bounce, pitch and roll modes of vehicle dynamics.

The parameter values for  $a, b, k_1, k_2, c_1, c_2$  and the amplitudes of excitation  $Y_1$  and  $Y_2$  are selected based on the actual experimental test values used in the next section to facilitate comparison of the theoretical results with the experimental ones. The parameter values used in this plot are  $Y = 0.005$  m,  $Z_{max} = 0.022$  m,  $\omega_n = \sqrt{k/m} = 7.56$  rad/s, where the stiffness  $k = 16$  kN/m and the mass  $m = 280$  kg. The tire parameter values are  $m_{tire} = m_{vehicle}/10$ ,  $k_{tire} = 8 * k_{suspension}$  and the tire damping is ignored. These parameter values correspond to those of the experimental setup discussed in the next section.

The average value of the power from the two wheels is used for the roll and pitch modes as the theoretical formula gives the sum of the values for two wheels.

The damping values used for numerical calculations are the same as those of viscous damping in the vehicle shock absorber system. This damping converts the kinetic energy of the suspension vibrations to heat and is wasted. The numerical calculations performed in this section are based on the assumption that when a regenerative system replaces the viscous damper it can potentially recover all the energy that would otherwise be wasted.

The theoretical potential amount of energy that can be harvested from vehicle suspensions was formulated in this section. In Section III, an experimental investigation is carried out to obtain the potential amount of energy that can be harvested from an actual vehicle associated with the dynamic modes of the vehicle explored in the theory section. The harvested power from the experiment is the power dissipated by linear damper, which is also maximum ideal harvestable power.

## III. EXPERIMENTAL INVESTIGATION OF THE OUTPUT POWER

The potential amount of energy that can be harvested associated with bounce, pitch and roll modes of vehicles is investigated in this section experimentally. This can represent the physical limits of the system in terms of the maximum amount of energy that can be harvested from suspension

vibrations, if there is no energy loss in the energy harvester system, while maintain at least the same ride comfort as a viscous damper in a regular vehicle suspension system (with no active vibration control). The road simulator rig shown in Fig. 4 has four hydraulic actuators. The vehicle is suspended on the hydraulic actuators which act as shakers for simulating road conditions and exciting the vehicle in bounce, pitch and roll modes of vehicle vibration. Fig. 4 also shows the front and rear suspension setups and the locations of the accelerometers, LVDTs (Linear variable differential transformers) and shakers.

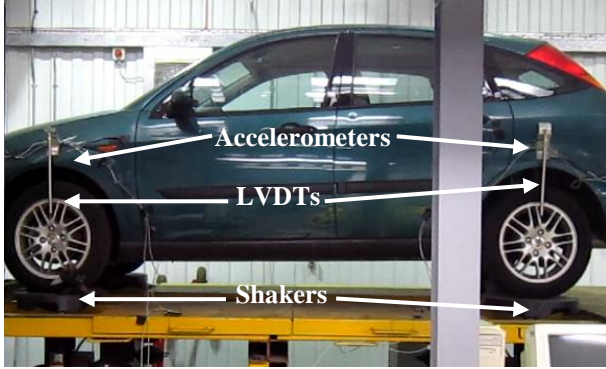


Fig. 4. The experimental setup for measuring the energy associated with bounce, pitch and roll modes of vehicle dynamics for potential harvesting.

The displacement of the center of each wheel is measured relative to the vehicle body using LVDTs. This relative displacement is denoted by  $z$  in the theoretical formulations given in Section II. A frequency sweep of 0.5 Hz to 20 Hz is applied to the tires by the shakers for a duration of 40 seconds. The vehicle used in this experiment is a Ford Focus with a total mass  $M = 1120$  kg, pitch moment of inertia of  $I = 1720$  kg.m<sup>2</sup> about the center of gravity of the vehicle, front suspension stiffness  $k_1 = 16$  kN/m, and rear suspension stiffness  $k_2 = 20$  kN/m. The calibration factor of the LVDTs is 150 mV/mm. The peak to peak displacement of the input excitation can be set to a desired value. The peak to peak input displacement excitation applied by the shaker is denoted by  $Y$  in the theoretical analysis given in Section II. In this experiment, this displacement amplitude is set to 10 mm.

The potential power that can be harvested by each shock absorber is equal to the power associated with the viscous dampers, which is normally dissipated and hence wasted. This power level can be calculated using Equation (2), as

$$P = c\dot{z} \times \dot{z} = 2\zeta m\omega_n \dot{z}^2 \quad (6)$$

For the test vehicle, the damping ratio of the viscous damper is  $\zeta = 0.3$ , and the natural frequency of the quarter-car model is  $\omega_n = (m/k)^{1/2} = 7.56$  rad/s. The velocity  $\dot{z}$  is calculated using the experimental  $z$  values as measured by the LVDTs, where  $\dot{z} = \frac{z_n - z_{n-1}}{t - t_{n-1}}$  and  $z_n$  denotes the relative displacement at time  $t_n$ . Therefore, the harvested power corresponding to the bounce, pitch and roll modes of the vehicle dynamic is calculated using the parameters given above and Equation (6). Each hydraulic actuator in the vehicle shaker rig can be programmed to vibrate independently of the other shakers in order to simulate any road condition and any vehicle mode of vibration. The power output for each mode is presented next.

#### A. The Bounce Mode

When all four shakers vibrate in phase with the same frequency and amplitude, the rig simulates the vehicle's bounce mode of vibration. The power that can be potentially generated by each shock absorber is calculated using the measured relative displacements and Equation (6). This power is shown in Fig. 5.

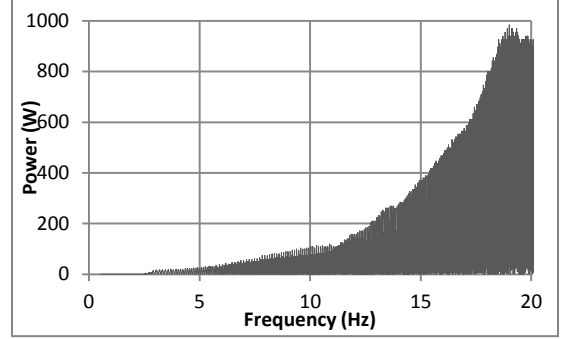


Fig. 5. The potential experimentally generated power from the suspension associated with the bounce mode of the vehicle as a function of excitation frequency.

#### B. The Pitch Mode

The pitch dynamic mode can be generated by the experimental rig when two front shakers of the vehicle move out of phase relative to the two rear shakers. The possible power generation associated with the pitch mode using Equation (6) and the vehicle parameters is presented in Fig. 6. This power is the sum of the power generated by the two front shock absorbers. The maximum value of the power at the excitation frequency of 20Hz is equal to 1482 W. Hence, the average value for just one wheel is 741 W.

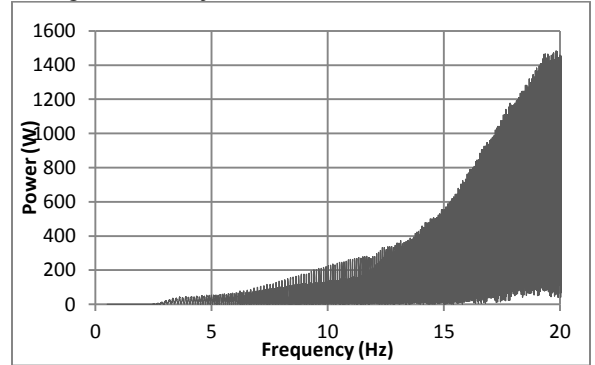


Fig. 6. The potential experimentally generated power by the two front shock absorbers associated with the pitch mode of the vehicle as a function of excitation frequency.

#### C. The Roll Mode

In the experimental rig, the roll mode is simulated when the two shakers on the right side of the vehicle move out of phase relative to the two shakers on the left side. The possible power level that can be generated in the roll mode is obtained using Equation (6). The power is calculated as the sum of the two power values generated by the two shock absorbers on the right side of the vehicle. The maximum value of the power at excitation frequency 20Hz is equal to 1572W.

Hence, the average value for just one wheel is given by 786 W.

A peak to peak input displacement ( $Y$ ) of 10 mm is applied by the shakers for producing the presented results. The possible power generation associated with 6 mm and 8 mm peak to peak maximum displacements, applied by the shaker, shows maximum power of 350 W and 600 W, respectively at 20 Hz excitation frequency. The maximum amplitudes 6mm, 8mm and 10mm of input displacement applied by the shaker rig correspond to a typical city road profile.

Table I presents a comparison between the experimentally generated power as given in the present section and the corresponding theoretical values determined in Section II. The power values reported in this table are for an excitation frequency of 20 Hz.

TABLE I  
COMPARISON BETWEEN THE THEORETICAL AND EXPERIMENTAL POWER VALUES

Dynamic Mode	Theoretical Power (W)	Experimental Power (W)	Difference (%)
Bounce	1106	984	11%
Pitch	880.5	741	15.8%
Roll	974.5	786	19.3%

The theoretical and experimental power values in Table I are in reasonable agreement. The theoretical approach presented in Section II is aimed to give the general analytical formulation for the maximum potential energy available from suspension, when the energy harvesting system is lossless. This theoretical model is not meant to provide the exact model of any particular vehicle (e.g. the Ford Focus in this paper). There are various parameters in the theoretical model that are not identical to the experimental parameters. The tire damping is ignored in the theoretical models. For a vehicle, typical tire damping values are in the range of 6% to 7% [32]. Nonlinearities (e.g. due to spring and connections), which are neglected in the theoretical models. Therefore the comparison made in Table 1 is to only give a degree of confidence and certainly that the theory and experiment are in agreement in terms of exhibiting comparable energy versus frequency curves, and not to calculate errors between the theoretical and experimental results.

The experimental power values obtained in this section correspond to those that can be potentially available from each suspension unit of the vehicle. The actual useful power that can be generated using a regenerative shock absorber is discussed in the next section.

The theoretical formulations in Section II and the experimental results in this section give the maximum or potential amount of energy that can be harvested associated with bounce, pitch and roll modes of vehicle dynamics. This represents the physical limits of the system in terms of the amount of energy harvesting from suspension vibrations, in the absence of any energy loss in the energy harvester, while maintain the same ride comfort as a regular shock absorber with no active vibration control. In the following section, a regenerative actuator is developed for suspension energy harvesting which can represent the actual amount of energy that can be harvested.

#### IV. THE REGENERATIVE ACTUATOR

The experimental and theoretical results in the previous sections provide the maximum potential amount of energy that can be harvested from the vehicle suspension with a lossless energy harvester. In this section, the actual energy that can be harvested by an actual physical regenerative actuator system is explored. The regenerative experimental rig is shown in Fig. 7. The main components of this experimental rig are a shaker, a regenerative actuator, springs, accelerometers, weights, power supply and power measurement setup. A mass of 50kg was vertically supported on the regenerative actuator. The base of the regenerative actuator is excited with a sinusoidal oscillation as applied by the shaker.

The rig shown in Fig. 7 contains the regenerative shock absorber shown in Fig. 8, which is an Exlar GSX20-0304 unit with a stroke of 2 in, screw lead of 0.4 in, maximum velocity of 33.33 in/sec, maximum static load of 1250 lb, and a dynamic load rating of 1230 lb.

In a regenerative shock absorber there is a regenerative actuator (Fig. 8) in place of the viscous damper of the suspension system. The regenerative actuator converts the kinetic energy of vehicle vibration into electrical energy. The springs in the original suspension system remain in the regenerative system. The theoretical representation of this system in terms of energy harvesting is given in Section V. The vibration model can be presented as in the bounce mode given in Section II. However this section gives the actual power rather than the lossless theoretical energy amount reported earlier.

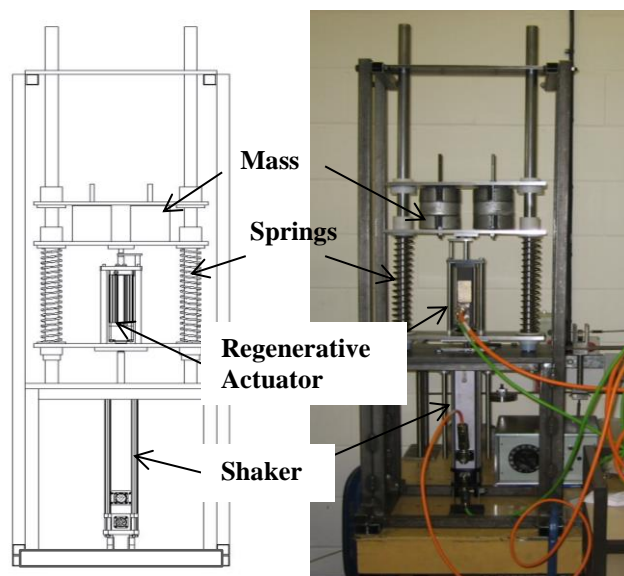


Fig. 7. The regenerative actuator of a quarter-vehicle model.

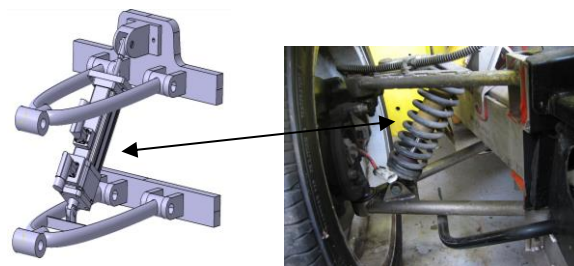


Fig. 8. Regenerative actuator that replaces the viscous damper of a shock absorber.

Power measurement and data acquisition used in the experimental regenerative system in Fig. 7 are discussed next.

#### A. Data Acquisition

In the experimental setup of Fig. 7, the power output of the regenerative actuator is applied to a load resistor through a 3 phase rectifier to convert the 3 phase ac (alternating current). The power output is calculated using the current through the load resistor,  $R_l$ . The National instruments NI cDAQ-9174 modular system is used as the data acquisition system in the experimental setup. A modular system with external power supply was chosen for its versatility and high data capture rate. Of the 4 slots available, the NI-9215 analog input module and NI-9234 IEPE (integrated electronic-piezoelectric) is used to input the necessary data in the experiment. The NI-9215 monitors the current passing through the load resistor, which is used to calculate the regenerated power, and the NI-9234 acquires acceleration of the road profile and mass which is later analyzed for determining the oscillation phase angle, an indicator of the relative wheel travel.

#### B. Power Measurement

The current is measured using an LEM LTSP25-NP current transducer. Fig. 9 presents the circuit diagram of the setup, where a load resistance of  $100\Omega$  is used. The output current is passed through an RMS filter. The power generated by the regenerative actuator is determined from the resistance value and the measured current using the formula  $P = I^2R$  in LabView software.

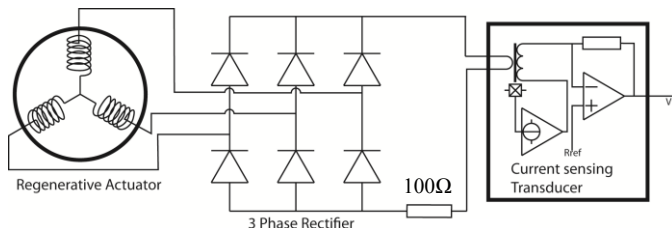


Fig. 9. Circuit diagram of the experimental circuitry for obtaining the current and generated power.

The generated power is plotted in Fig. 10. It should be noted that this is a scaled experiment, and therefore in order to obtain the level of power harvested by a vehicle, the mass and the relative displacement between the mass and the shaker input should be scaled to actual vehicle parameters.

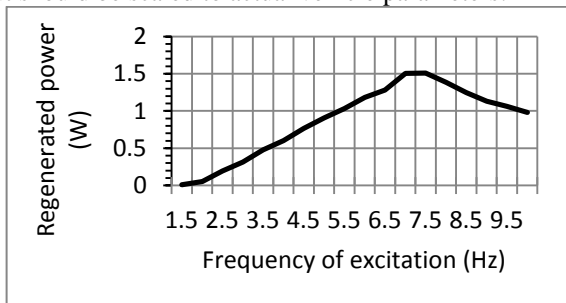


Fig. 10. Power regeneration rate versus excitation frequency.

The limitations of the equipment in the experimental rig in Fig. 7, mainly due to the limits of shaker displacement, do not allow further increase in the harvested power. The power harvesting electronics can be optimized to increase the harvested power. For instance, by manipulating the load resistance at various frequencies, the generated power can be maximized. The theoretical and experimental power values reported in the previous sections were based on the power that is potentially available, which does not consider the efficiency of the regenerative system. Therefore, as expected, the harvested power as determined in this section is relatively lower than the theoretical and potential power values reported in the previous sections.

Further issues regarding the shaker and the experimental setup are addressed now. Considering a sinusoidal road profile, the frequency of the sine wave was swept from 1 Hz to 10Hz. Due to the setup conditions, the amplitude could not be sustained by the shaker actuator. The frequency sweep allows for power spectrum analysis across a range of excitation frequencies. The actuator was unable to operate at excitation frequencies over 10Hz. The initial movement from a standstill was found to have a back drive force. This effect was found to increase with applied lower resistive load, and would be magnified by the lead pitching of the screw.

#### C. System Implementation

Modifying an existing suspension system to implement a new concept should be done by ensuring minimal change to the driving behavior (possibly positive). Therefore, a commonly found suspension type is reverse engineered to establish the required modification prior to fitting the regenerative actuators in place of a conventional damper system. A regenerative actuator linked to an on-board controller allows for active suspension control while regenerating additional power for on board needs. Fig. 8 presents a CAD model for implementing a regenerative shock absorber in the suspension system. The regenerative actuator used in this experiment is an Exlar GSX20-0304 model. This linear actuator includes an inverted roller screw design offering a very long life cycle compared to an equivalent ball screw design (typically 15 times more travel life in the X grade and 5 times more in the M grade). Roller Screw actuators can also offer much higher speeds and forces in a more compact physical package, compared to their ball screw equivalents. They are also quieter which is a plus in terms of health and safety. Roller screw actuators are much more robust and can withstand much greater shock loading than ball screw actuators. They have lower inertia so can be accelerated faster using less current & power. The efficiency of this actuator is 80%. The suspension concept in Fig. 8 is designed around the dimensions of this actuator.

#### D. Reliability and useful life

Life expectancy of a regenerative actuator as a shock absorber depends on various factors. According to the GSX20 actuator data sheet, the prediction of life can be made when the linear travel distance in the roller screw of the actuator is within the designed limit. For an L10 roller screw linear actuator, the travel life in millions of inches is obtained as

$$L_{10} = (C/F)^3 \times S \quad (7)$$

where  $C$  denotes dynamic load rating (lbf),  $F$  is the cubic mean applied load (lbf) and  $S$  is the lead (inches) of the roller screws. The travel life curve, in millions of inches and mm, is supplied by the actuator manufacturer in terms of mean load pounds (N). For instance, for a GSX20, when the applied load is 500N (an estimate for the 50 kg weight in the experiment in Fig. 7) the travel life is 6 million inches.

The above sections discussed the amount of energy that can be harvested from vehicle suspension. The application of this harvested energy in a vehicle system is discussed below in order to explain why a regenerative system is required and how the harvested energy is utilized.

## V. SELF-POWERED ACTUATION

The application of the suspension energy harvesting is to supply power input for active vibration control and/or to be stored as power source for other energy demand in the vehicle. It should be noted that the energy harvesting system is not designed to only maximize the amount of energy that can be harvested. It is designed to harvest energy while maintaining at least the same ride comfort and handling of a regular suspension system. If the harvested power used for vibration control applications then it should provide a better ride comfort and handling than a suspension systems that is not equipped with the energy harvesting systems.

The application of energy harvesting can be viewed both in a 'regenerative only' scheme and in a self-powered scheme. In a regenerative scheme the generated electrical energy is stored and is available as a power source for various uses in the vehicle. In the self-powered scheme, the system generates electrical energy from vibration and feeds the generated electrical power back into an actuation system to control the same vibration that regenerates the electrical energy. For instance, in a self-powered shock absorber, the system supplies the regenerated power to drive the actuator itself for controlling the vehicle vibrations. The theoretical expressions of the regenerative and self-powered schemes are obtained now.

### A. The regenerative scheme

In the 'regenerative only' scheme the power is stored and supplied as an electrical power source for any required application in the system.

In a linear actuator, the relationship between the induced voltage,  $V$ , and velocity,  $\dot{z}$ , can be expressed in terms of the motor constant,  $k_a$ , by [15] and [33]:

$$V = -k_a \dot{z} \quad (8)$$

and the motor force,  $F$ , is obtained in terms of current in the armature by the following expression.

$$F = k_a i \quad (9)$$

Using Equations (8) and (9), the force in the actuator can be obtained in term of velocity by

$$F = -\frac{k_a^2}{r} \dot{z} \quad (10)$$

where  $r$  is the resistance of the armature.

If Equation (10), is compared with the force-velocity relation in a viscous damper ( $F = c\dot{z}$ ), then the equivalent damping (as introduced in Sections II and III) of the motor is

$$c_{eq} = -\frac{k_a^2}{r} \quad (11)$$

Thus the power for the case of the 'regenerative only' case can be obtained as given by Equation (2).

$$P = c_{eq} \dot{z}^2 = -\frac{k_a^2}{r} \dot{z}^2 \quad (12)$$

### B. The self-powered scheme

In the self-powered scheme, the system generates electrical energy from vibration and feeds the generated electrical power back to the actuation system to drive the actuator. Therefore the actuator is capable of controlling the same vibration which is being regenerated to electrical energy, as a self-powered dynamic system [29].

If the voltage of the power source that generates actuation is  $V_p$  then the force in the actuator is determined by

$$F = k_a \frac{V_p - k_a \dot{z}}{r} \quad (13)$$

Generating the actuation force,  $F$ , consumes power,  $P_c$ , given by

$$P_c = V_p i = \left( \frac{rF}{k_a} + k_a \dot{z} \right) \frac{F}{k_a} \quad (14)$$

From Equations (12) and (14), the consumed power can be written in terms of the equivalent damping as

$$P_c = \frac{1}{c_{eq}} F^2 + F \dot{z} \quad (15)$$

where  $c_{eq} = 2\zeta\omega_n m$ , for  $\zeta = 0.3$  and  $\omega_n = (k/m)^{1/2}$ .  $c_{eq}$ ,  $\omega_n$  and  $\zeta$  values are chosen corresponding to the vehicle parameters in the experimental section (Section III), for a quarter of the vehicle model.

If parameter  $\lambda$  is considered as (for  $\dot{z} \neq 0$ ) [15]

$$\lambda = \frac{F}{-c_{eq} \dot{z}}$$

then, the power consumption in Equation (15) can be rewritten as

$$P_c = c_{eq} \dot{z}^2 \lambda (\lambda - 1) \quad (16)$$

$P_c$  in Equation (16) is plotted versus  $\lambda$  and  $\dot{z}$  in Fig. 11.

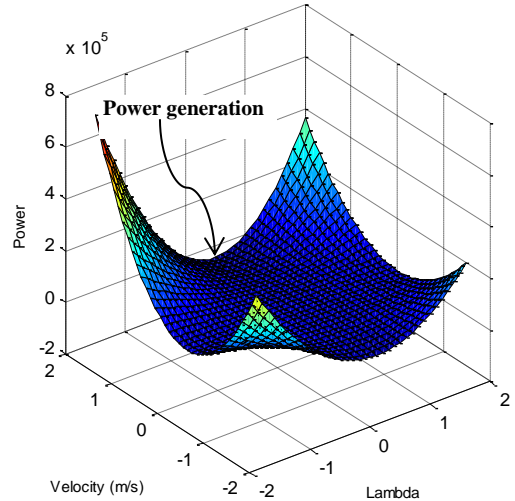


Fig. 11. Power (W) versus Lambda and Velocity [29].



The region of the surface in Fig. 11 where  $P_c < 0$  (where the values of the power is negative) corresponds to the power generation state, and the positive values correspond to power consumption by the system.

The plot in Fig. 12 demonstrates the normalized power,  $P_c/c_{eq}\dot{z}^2$ , versus  $\lambda$ . The region of the surface where  $P_c/c_{eq}\dot{z}^2 < 0$  (where the normalized power is negative) corresponds to the power generation state, and the positive values correspond to power consumption by the system.

For  $|F| < |c_{eq}\dot{z}|$ , or  $0 < \lambda < 1$  region in Fig. 11 and Fig. 12, the required force to drive the actuator is less than the dynamic force in the actuator. Where the dynamic force,  $c_{eq}\dot{z}$ , is due to the kinetic energy of the actuator motion. Therefore the kinetic energy can be converted to electrical energy. This electrical energy is fed back to the actuator system which generates the actuation driving force to control the vibration, as a self-powered mechanism. It should be noted that there is no guarantee that the harvested energy is sufficient to control the entire range of vibration level. In this case, the self-powered system should be capable of accumulating the energy and then supply the sufficient level of energy to drive the actuator.

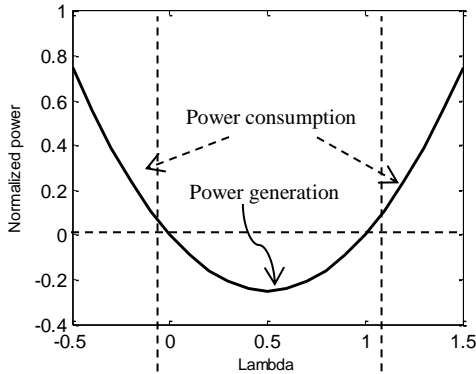


Fig. 12. Normalized power versus Lambda [29].

It follows that the levels of power generation and power consumption can be explained using Equations (15) and (16), and Fig. 11 and Fig. 12. As discussed above, in the self-powered mode the system feeds the generated power back to the system to drive the actuator and control the same vibration that generates electrical energy. However, a self-powered design can be a more cost effective option relative to a 'regenerative only' option. Furthermore a self-powered actuation may not be a preferred option where the actuation system provides acceptable performance. For instance, the actuator equivalent damping provides sufficient damping for a shock absorber system for reducing vehicle vibration. In this case the harvested energy will be stored in a battery or an ultra/supercapacitor for other electrical energy demands in the vehicle. This section discussed the application of energy harvesting for vibration control and other energy demands of the vehicle. The design of a control system of an active suspension can be achieved using various control strategies (e.g. [13]-[17]). For instance, the variable load resistor discussed in Section IV can be adjusted for vibration control purposes. This is discussed briefly in the next section for analysis of ride comfort and road handling.

## VI. THE EFFECT OF ENERGY EXTRACTION ON RIDE COMFORT AND ROAD HANDLING

It is required to investigate the effect of energy extraction, for suspension energy harvesting and self-powered actuation, as discussed in Section V, on the vehicle ride comfort and road handling. In the following sections, the analysis of ride comfort and road handling is investigated in association with the suspension energy regeneration, and then the effect of real road profile on energy harvesting, road handling and ride comfort is addressed. The model used in this section for ride comfort, vehicle handling and energy harvesting analyses corresponds to the 2DOF model in Fig. 1 and the energy harvesting formulation given by Equation (3).

### A. Control parameters

It is required to maintain ride comfort of a vehicle while harvesting energy from the suspension system. If a skyhook controller is implemented for providing ride comfort the applied force by the actuator produces a damping force expressed as

$$f = c_{skyhook}\dot{x}_1 \quad (17)$$

where  $c_{skyhook}$  is the feedback gain of the controller, and  $\dot{x}_1$  is the velocity associated with  $x_1$  in figure 1. Equivalent damping of a regenerative actuator without any control mechanism is given by  $c_{eq}$  in Equation (11).

Controlling the suspension for providing the ride comfort can be analyzed in terms of the skyhook feedback gain as a factor of the equivalent damping of the actuator using constant  $n$  as follows.

$$c_{skyhook} = n c_{eq} \quad (18)$$

The controller can adjust  $c_{skyhook}$  for various excitation frequencies using a variable resistance. The controller is designed to manipulate the parameter  $n$  in Equation (18), using a variable resistance, where the value of  $n$  is proportional to the inverse of the resistance in Equation (11)

$$n \propto 1/r \quad (19)$$

Fig. 13 shows the result of variable resistance on equivalent damping using Equation (11). The value for the motor constant,  $k_a$ , used in the calculations is equal to 209.6 Volts/m/s, corresponding to Exlar GSX20-0304 actuator in Section IV. For  $r=35 \Omega$ , the corresponding equivalent damping (from Fig. 13) can be obtained as  $c_{eq}=1270 \text{ N/m/s}$ . This damping value is equal to the vehicle suspension damping given by the parameters in Section III and Equation (6).

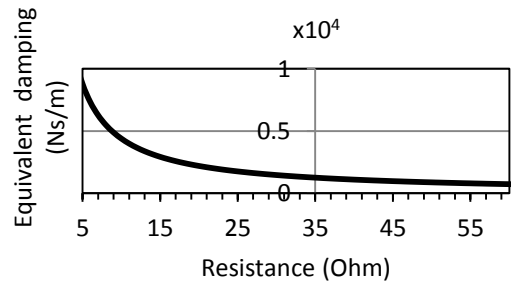


Fig. 13. Variable resistance for the skyhook controller.

Therefore in a regenerative suspension system, the damping can be manipulated by varying the resistance (Equations (18) and (19)) in order to provide better ride comfort, road dandling or energy regeneration. It should be noted that the battery load that stores the electrical energy can be considered as part of this resistance and therefore the amount of stored electrical energy in the battery plus the wasted energy in the variable resistance is equal to the total mechanical work done by the actuator (when the actuator generates energy).

### B. Ride comfort

In order to study the ride comfort of a vehicle equipped with regenerative suspension systems, acceleration response of the vehicle body to road excitations is analyzed. Acceleration of the vehicle body for various values of  $n$  (Equations (18) and (19)) is given in Fig. 14. As seen from the figure, higher damping values (e.g. when  $n = 5$ ) is favorable at lower excitation frequencies, and lower damping (e.g. when  $n = 0.5$ ) is desirable for high excitation frequency.

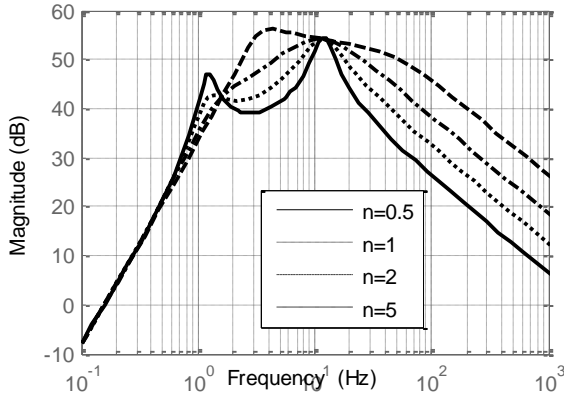


Fig. 14. Acceleration of the sprung mass  $m_1$  for various values of  $n$ .

### C. Vehicle handling

If the displacement of the tire subjected to random road excitations is equal to static deflection of the tire, the force between the road and the tire becomes zero. This is unfavorable for vehicle road handling. The static deflection of the tire can be obtained from Fig. 1 as

$$x_0 = (m_1 + m_2)/k_2$$

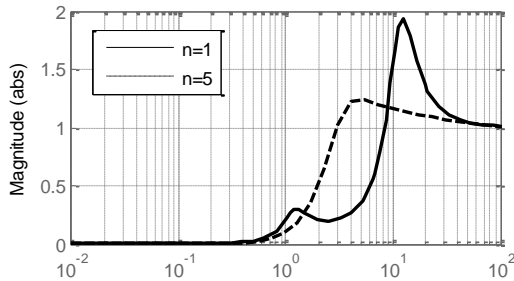


Fig. 15. Tire deflection for  $n = 1$  and 5.

The value of the static tire deflection for the vehicle parameters used in this paper is equal to  $x_0 = 0.0024$  m. The response of the tire displacement is given in Fig. 15 for  $n=1$  and 5.

It is shown in Fig. 15 that for high and low excitation frequencies the damping condition corresponding to  $n=1$  is favorable as it gives larger tire deflection. Random vibration analysis result gives the RMS value of tire deflection equal to 0.0027m for  $n=1$ , and gives RMS tire deflection result of 0.0032m for  $n=5$ . These tire deflection values are larger than the static tire deflection which is suitable for road handling.  $n=5$  gives a better road handling due to larger tire deflection relative to  $n=1$  case in this numerical example.

### D. Discussions on the effects of energy extraction on dynamics of vehicles

The logarithmic values of the harvested energy versus frequency is plotted in Fig. 16. It should be noted that this is a Bode Plot and corresponds to the plot of a transfer function and not the actual power where the transfer function is obtained from Equation (2) as Power/(Input displacement squared). It is shown that larger damping is favorable for energy harvesting. However as it was shown in the previous sections this is not always the case for ride comfort and road handling. Table II summarizes the effect of damping (or control parameter  $n$ , or variable resistance) on ride comfort (analyzed by acceleration), road handling (analyzed tire deflections), and energy harvesting.

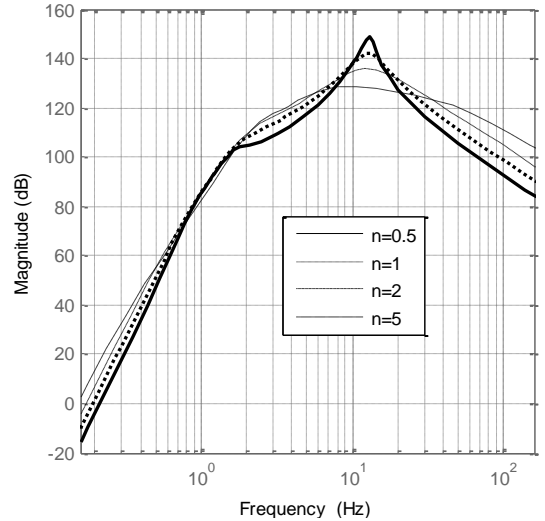


Fig. 16. The harvested energy (logarithmic) from suspension versus frequency (logarithmic).

TABLE II  
THE EFFECT OF DAMPING ON RIDE COMFORT, ROAD HANDLING AND ENERGY HARVESTING

Frequency range	Low frequency	Mid frequency	High frequency
Acceleration, $\ddot{x}_1$ (smaller better for ride comfort)	$\ddot{x}_1(n=5) <$ $\ddot{x}_1(n=0.5)$	$\ddot{x}_1(n=0.5) <$ $\ddot{x}_1(n=5)$	$\ddot{x}_1(n=0.5) <$ $\ddot{x}_1(n=5)$
Tire deflection, $x_0$ (Larger better for road handling)	$x_0(n=1) >$ $x_0(n=5)$	$x_0(n=5) >$ $x_0(n=1)$	$x_0(n=1) >$ $x_0(n=5)$
	Higher damping better	Lower damping better	Lower damping better
	Lower damping better	Higher damping better	Lower damping better

Power regeneration, $P$	$P(n=5) > P(n=0.5)$	$P(n=5) > P(n=0.5)$	$P(n=5) > P(n=0.5)$
	Higher damping better	Higher damping better (Except at the natural frequency)	Higher damping better

Therefore an optimized value of control parameter is required to be determined in order to design for an optimum value of energy harvesting while maintaining the ride comfort and acceptable road handling levels.

### E. Random excitations

To obtain a realistic level of ride comfort, the acceleration is obtained when input excitations to the vehicle is expressed by power spectral density (PSD) function of random road surface profile proposed by ISO [31], [34]-[35]. The PSD of a road surface can be expressed as a function of spatial frequency as [31]

$$S_g(\Omega) = C_{sp}\Omega^{-N} \quad (20)$$

where  $S_g(\Omega)$  is the PSD function of the road elevation,  $\Omega$  denotes the special frequency, and  $C_{sp}$  and  $N$  are constants given by the below for a smooth highway

$$N = 2.1$$

$$C_{sp} = 4.8 \times 10^{-7}$$

Fig. 17 represents the PSD input excitation for a smooth highway used here for ride comfort analysis.

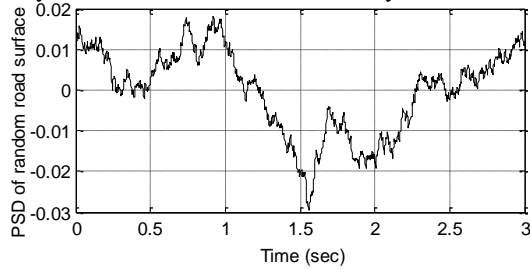


Fig. 17. PSD of a road profile.

Fig. 18 represents the relative velocity of the sprung mass  $m_1$  with respect to unsprung mass  $m_2$  for the bounce model in Fig. 1 when the system is subjected to the random road excitation in Fig. 17. This relative velocity is responsible for regeneration of energy. The same parameter values for stiffness and mass values are used as given in Part C for numerical analysis. The RMS value of the relative velocity is 0.1356 m/s.

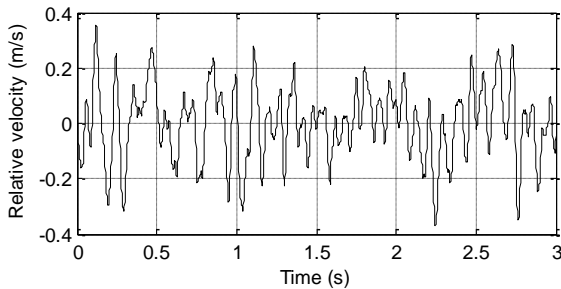


Fig. 18. Relative velocity of the sprung mass  $m_1$  with respect to unsprung mass  $m_2$  for a bounce model when subjected to the random road profile.

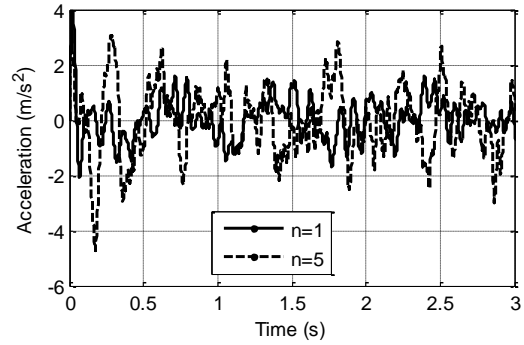


Fig. 19. Vehicle acceleration response to smooth highway profile for  $n = 1$  and  $n = 5$ .

Fig. 19 illustrates the acceleration response of the vehicle body to the smooth highway profile in time domain. For  $n = 1$ , the RMS value of the acceleration is  $0.7715 \text{ m/s}^2$  and for  $n = 5$ , the acceleration RMS is  $1.2893 \text{ m/s}^2$ , which agree with the results in Fig. 14 for higher excitation frequency range as the vehicle speed is 30 m/s in this simulation.

Fig. 20 demonstrates the numerical results of the harvested energy by the regenerative suspension when subjected to the random road profile in Fig. 17 and with the vehicle speed equal to 30 m/s. The RMS value of the harvested energy in this analysis is 42.39 W for  $n=5$ , and 40.47 W for  $n=1$ .

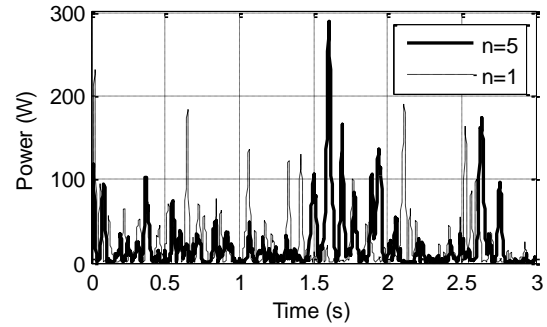


Fig. 20. The harvested energy from suspension when subjected to the random road profile for  $n=1$  and  $n=5$ .

## VII. CONCLUSION

The main contribution of the paper includes the theoretical and experimental investigation of the potential amount of energy that can be harvested associated with the bounce, pitch and roll mode of vehicle dynamics, using a regenerative system. The paper also discusses the actual amount of energy that can be harvested by a regenerative actuator system using a quarter-vehicle experimental rig, explains the application of energy harvesting for self-powered actuation, and addresses the effect of energy harvesting on ride comfort and road handling.

As a future work, this investigation can be extended to energy harvesting of a 7DOF dynamic model with coupled modes of vibration.

## ACKNOWLEDGMENT

Farbod Khoshnoud thanks Karen Craddock, Program Manager, Environmental Sciences Department at Defence Science and Technology Laboratory (DSTL), and Neil Service, from Physical Sciences Department, Platform

Sciences Group at DSTL, for their very helpful suggestions and comments during the research carried out in this paper.

## REFERENCES

- [1] D. Karnopp, "Permanent Magnet Linear Motors Used as Variable Mechanical Dampers for Vehicle Suspensions," *Vehicle System Dynamics*, 18, pp. 187–200, 1989.
- [2] D. Karnopp, "Power Requirement for Vehicle Suspension Systems," *Vehicle System Dynamics*, 21(1), pp. 65–71, 1992.
- [3] L. Segel and X.-P. Lu., "Vehicular Resistance to Motion as Influenced by Road Roughness and Highway Alignment," *Australian Road Research*, 12(4), pp. 211–222, 1982.
- [4] P. Hsu, "Power Recovery Property of Electrical Active Suspension Systems," *Proceedings of the 31st Intersociety Energy Conversion Engineering Conference, (IECEC 96)*, Washington, DC, August 11–16, 1996, pp. 1899–1904.
- [5] A. Abouelnour and N. Hammad, "Electric Utilization of Vehicle Damper Dissipated Energy," *Al-Azhar Engineering Seventh International Conference (AEIC)*, Cairo, Egypt, April 7–10, 2003.
- [6] R. Goldner, P. Zerigian and J. Hull, "A Preliminary Study of Energy Recovery in Vehicles by Using Regenerative Magnetic Shock Absorbers," *SAE Paper No. 2001-01-2071*, 2001.
- [7] Y. Kawamoto, Y. Suda, H. Inoue and T. Kondo, "Modeling of Electromagnetic Damper for Automobile Suspension," *J. Syst. Des. Dyn.*, 1, pp. 524–535, 2007.
- [8] Y. Zhang, K. Huang, F. Yu, Y. Gu and D. Li, "Experimental Verification of Energy-Regenerative Feasibility for an Automotive Electrical Suspension System," *Proceedings of the IEEE International Conference on Vehicular Electronics and Safety*, Beijing, China, December 13–15, 2007.
- [9] L. Zuo, B. Scully, J. Shestani and Y. Zhou, "Design and characterization of an electromagnetic energy harvester for vehicle suspensions," *Smart Materials and Structures*, 19, 045003 (10pp), 2010.
- [10] L. Zuo and P. Zhang, "Energy harvesting, ride comfort and road handling of regenerative vehicle suspensions," *ASME Journal of Vibrations and Acoustics*, Vol. 135 / 011002-1, 2013.
- [11] Z. Li, L. Zuo, J. Kuang and G. Luhrs, "Energy-harvesting shock absorber with a mechanical motion rectifier," *Smart Materials and Structures*, 22, 025008 (10pp), 2013.
- [12] I. Martins, "Permanent-Magnets Linear Actuators Applicability in Automobile Active Suspensions", *IEEE Transactions on Vehicular Technology*, Vol. 55, pp. 86-94, 2006.
- [13] Y. Suda, S. Nakadai and K. Nakano, "Hybrid suspension, system with skyhook control and energy regeneration (Development of self-powered active suspension)," *Vehicle System Dynamics*, 19, pp. 619–34, 1998.
- [14] K. Nakano and Y. Suda, "Combined type self-powered active, vibration control of truck cabins," *Vehicle Systems Dynamics*, 41, pp. 449–73, 2004.
- [15] K. Nakano, Y. Suda and S. Nakadai, "Self-powered active vibration control using a single electric actuator," *Journal of Sound and Vibration*, 260, pp. 213–35, 2003.
- [16] Z. Li, L. Zuo, G. Luhrs, L. Lin, Y-x. Qin "Electromagnetic Energy-Harvesting Shock Absorbers: Design, Modelling and Road Tests," *IEEE Transaction on Vehicular Technology*, Vol. 62, No. 3, 2013.
- [17] Y. Okada, H. Harada and K. Suzuki, "Active and regenerative control of an electrodynamic-type suspension," *JSME international journal. Series C, Mechanical systems, machine elements and manufacturing*, 40(2), pp. 272-278, 1997.
- [18] S. S. Kim and Y. Okada, "Variable resistance type energy regenerative damper using pulse width modulated step-up chopper," *Journal of Vibration and Acoustics*, 124, 110–5, 2002.
- [19] D. Margolis, "Energy Regenerative Actuator for Motion Control With Application to Fluid Power Systems," *Journal of dynamic systems, measurement, and control*, 127(1), pp. 33-40, 2005.
- [20] M. R. Jolly and D. L. Margolis, "Assessing the potential for energy regeneration in dynamic subsystems," *Journal of dynamic systems, measurement and control, transactions of the ASME*, Volume: 119 Issue: 2, pp. 265-270, 1997.
- [21] M. R. Jolly and D. L. Margolis, "Regenerative systems for vibration control, *Journal of vibration and acoustics, transactions of the ASME*," Volume: 119 Issue: 2 pp. 208-215, 1997.
- [22] C. Nagode, M. Ahmadian, and S. Taheri, "Axle generator for freight car electric systems," *Proceedings of the ASME/ASCE/IEEE Joint Rail Conference*, Philadelphia, Pennsylvania, USA, 2012.
- [23] C. Nagode, M. Ahmadian, and S. Taheri, "Motion-based energy harvesting devices for railroad applications," *Proceedings of the Joint Rail Conference*, Urbana, Illinois, USA, 2010.
- [24] C. Nagode, M. Ahmadian, and S. Taheri, "Vibration-based energy harvesting systems for on-board applications," *Proceedings of the Joint Rail Conference*, Pueblo, Colorado, USA, 2011.
- [25] Y. Zhang, X. Zhang, M. Zhan, K. Guo, F. Zhao, and Z. Liu, "Study on a novel hydraulic pumping regenerative suspension for vehicles," *Journal of the Franklin Institute*, July 2014, ISSN0016-0032, <http://dx.doi.org/10.1016/j.jfranklin.2014.06.005>.
- [26] H. Zhang, X. Guo, L. Xu, S. Hu, and Z. Fang, "Parameters Analysis of Hydraulic-Electrical Energy Regenerative Absorber on Suspension Performance," *Advances in Mechanical Engineering*, Volume 2014, Article ID 836502, 2014.
- [27] A. Casavola, F. Di Iorio and F. Tedesco, "Gain-Scheduling Control of Electromagnetic Regenerative Shock Absorbers for Energy Harvesting by Road Unevenness," *American Control Conference*, June 4-6, Portland, Oregon, USA. 2014.
- [28] F. Khoshnoud, D. B. Sundar, M. N. M. Badi, Y. K. Chen, R. K. Calay, and C. W. De Silva, "Energy harvesting from suspension systems using regenerative force actuators," *International Journal of Vehicle Noise and Vibration*, Vol. 9, Nos. 3/4, pp. 294 - 311, 2013.
- [29] F. Khoshnoud, Y. K. Chen, R. K. Calay, C. W. de Silva, H. Owahdi, "Self-Powered Dynamic Systems," *European Conference for Aeronautics and Space Sciences*, Munich, Germany, Paper No. 275, 1-5 July, 2013.
- [30] N. Stephen, "On energy harvesting from ambient vibration. *Journal of Sound and Vibration*," 293, pp. 409–425, 2006.
- [31] J. Y. Wong, *Theory of Ground Vehicles* (third edition), John Wiley & Sons, Inc, 2001.
- [32] A. G. Thompson, "The effect of tyre damping on the performance of vibration absorbers in an active suspension," *Journal of Sound and Vibration*, Volume 133, Issue 3, p. 457-465, 1989.
- [33] C. W. De Silva, "Mechatronics—A Foundation Course," CRC Press/Taylor&Francis. Boca Raton, FL, 2010.
- [34] De Silva, C.W., *Vibration Fundamentals and Practice* (Second Edition), CRC Press, Boca Raton, FL, 2007.
- [35] K. V. Inamdar, *Vehicle Suspension optimization for stochastic inputs*, M.S. Project, University of Texas, Arlington, 2011.